

# Sarcoplasmic Reticulum $\text{Ca}^{2+}$ Release Declines in Muscle Fibers from Aging Mice

Ramón Jiménez-Moreno,\* Zhong-Min Wang,\* Robert C. Gerring,\* and Osvaldo Delbono\*<sup>†‡</sup>

\*Department of Physiology and Pharmacology, <sup>†</sup>Department of Internal Medicine, Section on Gerontology, and <sup>‡</sup>Neuroscience Program, Wake Forest University School of Medicine, Winston-Salem, North Carolina

**ABSTRACT** This study hypothesized that decline in sarcoplasmic reticulum (SR)  $\text{Ca}^{2+}$  release and maximal SR-releasable  $\text{Ca}^{2+}$  contributes to decreased specific force with aging. To test it, we recorded electrically evoked maximal isometric specific force followed by 4-chloro-m-cresol (4-CmC)-evoked maximal contracture force in single intact fibers from the mouse flexor digitorum brevis muscle. Significant differences in tetanic, but not in 4-CmC-evoked, contracture forces were recorded in fibers from aging mice as compared to younger mice. Peak intracellular  $\text{Ca}^{2+}$  in response to 4-CmC did not differ significantly. SR  $\text{Ca}^{2+}$  release was recorded in whole-cell patch-clamped fibers in the linescan mode of confocal microscopy using a low-affinity  $\text{Ca}^{2+}$  indicator (Oregon green bapta-5N) with high-intracellular ethylene glycol-bis( $\alpha$ -aminoethyl ether)- $N,N,N',N'$ -tetraacetic acid (20 mM). Maximal SR  $\text{Ca}^{2+}$  release, but not voltage dependence, was significantly changed in fibers from old compared to young mice. Increasing the duration of fiber depolarization did not increase the maximal rate of SR  $\text{Ca}^{2+}$  release in fibers from old compared to young mice. Voltage-dependent inactivation of SR  $\text{Ca}^{2+}$  release did not differ significantly between fibers from young and old mice. These findings indicate that alterations in excitation-contraction coupling, but not in maximal SR-releasable  $\text{Ca}^{2+}$ , account for the age-dependent decline in intracellular  $\text{Ca}^{2+}$  mobilization and specific force.

## INTRODUCTION

A basic problem common to aging mammals is diminished muscular strength. The many factors that account for absolute force in relation to lost muscle mass have been extensively reviewed (1–3) and probably are not directly related to age-related loss in the force-generating capacity of the skeletal muscle per cross-sectional area, or specific force (SF). In vitro studies on contractility showed that when the maximal isometric force for aged mice and rats is normalized to the smaller muscle fiber cross-sectional area, a significant deficit in specific isometric force remains unexplained by the smaller cross-sectional area (4–6). These data suggest that, in addition to reduced cross-sectional area, other factors contribute to muscle weakness in aged mammals; for example, contraction-induced injury (7), posttranslational modifications of contractile proteins (8), and excitation-contraction uncoupling (ECU) (9).

Excitation-contraction coupling (ECC) is a series of ionic and molecular events by which membrane depolarization is converted into skeletal muscle contraction. Two important proteins involved in ECC are the dihydropyridine receptor (DHPR) and the sarcoplasmic reticulum (SR) ryanodine receptor (RyR). Depolarization of the sarcolemma, associated with an action potential, causes charge movement within the

transverse tubules (10) and a conformational change in the DHPR (a voltage-gated  $\text{Ca}^{2+}$  channel/voltage sensor) (11). In skeletal muscle, the conformational change in the DHPR results in activation of the RyR at the triadic junction, causing  $\text{Ca}^{2+}$  release into the myoplasm and muscle contraction (12).

Peak intracellular  $\text{Ca}^{2+}$  transients evoked by sarcolemmal depolarization have been shown to decrease with age (9,13); however, whether alterations in sarcolemmal depolarization-evoked SR  $\text{Ca}^{2+}$  release and/or maximal SR-releasable  $\text{Ca}^{2+}$  account for this decrease is not known. This study was designed to determine whether the decreased  $\text{Ca}^{2+}$  transient in muscle fibers from old mice is due to decreased SR  $\text{Ca}^{2+}$  release and associated with diminished maximal SR-releasable  $\text{Ca}^{2+}$  in flexor digitorum brevis (FDB) muscle fibers.

In the past, the voltage dependence of the SR  $\text{Ca}^{2+}$  release flux in mammalian muscle fibers was inferred from theoretical deconvolutions of the evoked  $\text{Ca}^{2+}$  transients (14–18). Here, SR  $\text{Ca}^{2+}$  release was measured using a procedure applied to cardiac myocytes and FDB muscle fibers that combines a high intracellular ethylene glycol-bis( $\alpha$ -aminoethyl ether)- $N,N,N',N'$ -tetra-acetic acid (EGTA) concentration (20 mM) and a low-affinity  $\text{Ca}^{2+}$  indicator (Oregon green bapta-5N) with laser scanning confocal microscopy recordings (19–21). This approach allows direct measurement of the SR  $\text{Ca}^{2+}$  release flux from the recorded fluorescence transients.

We also took advantage of the potency and specificity of the RyR activator 4-chloro-m-cresol (4-CmC) (22–26) to elicit maximal SR  $\text{Ca}^{2+}$  release and force in single intact muscle fibers. Unlike caffeine, this compound has been shown to induce  $\text{Ca}^{2+}$  release via the RyR without adversely affecting the SR  $\text{Ca}^{2+}$  pump or myofibrillar sensitivity (23). It can therefore be used effectively to study the maximal force a

Submitted August 1, 2007, and accepted for publication December 3, 2007.

Ramón Jiménez-Moreno and Zhong-Min Wang contributed equally to this work.

Address reprint requests to Osvaldo Delbono, Dept. of Physiology and Pharmacology, Wake Forest University School of Medicine, 1 Medical Center Blvd., Winston-Salem, NC 27157. Tel.: 336-716-9802; Fax: 336-716-2273; E-mail: odelbono@wfubmc.edu.

Editor: David D. Thomas.

© 2008 by the Biophysical Society  
0006-3495/08/04/3178/11 \$2.00

doi: 10.1529/biophysj.107.118786

fiber can develop in response to maximal SR  $\text{Ca}^{2+}$  release, while bypassing the ECC mechanism.

The results of this study indicate that SR  $\text{Ca}^{2+}$  release is impaired, and maximal SR-releasable  $\text{Ca}^{2+}$  is preserved, which supports the ECU mechanism in aging muscle fibers. Preliminary results were presented at the 50th Annual Meeting of the Biophysical Society (Salt Lake City, UT, 2006).

## METHODS

### Animals

Flexor digitorum brevis muscles were dissected from young (3- to 6-month) and old (20- to 22-month) FVB (Friend virus B, our colony) or DBA (dilate brown agouti) mice. We have used these strains to study aging muscle (5,6,27), and availability determined the inclusion of the two strains in this work. However, the findings reported are independent of mouse strain (see below). The animals were housed at Wake Forest University School of Medicine and killed by cervical dislocation; animal handling and procedures were approved by the Wake Forest University School of Medicine Animal Care and Use Committee.

### Single intact fiber contraction and intracellular $\text{Ca}^{2+}$ recordings

The technique for dissecting single intact fibers followed procedures previously described (6,28). The recording solution consisted of (mM) NaCl 121, KCl 5,  $\text{CaCl}_2$  1.8,  $\text{MgCl}_2$  0.5,  $\text{NaH}_2\text{PO}_4$  0.4,  $\text{NaHCO}_3$  24, and glucose 5.5. Solutions were bubbled continuously with a mixture of 5%  $\text{CO}_2$ -95%  $\text{O}_2$  to achieve a pH of 7.4. The fiber was mounted between a 400A force-transducer (Aurora Scientific, Aurora, Ontario, Canada) (compliance, 1  $\mu\text{m mN}^{-1}$ ; resonant frequency, 0.6 kHz) and an adjustable holder, allowing control of fiber position and length, as described in previous studies (6,28). Fibers were stimulated by an electrical field generated between two parallel silver electrodes connected to a Grass S48 stimulator (Astro-Medical, West Warwick, RI). Fiber length was adjusted until maximal force was elicited by a single twitch contraction ( $L_0$ ) under isometric conditions. Suprathreshold square wave pulses of 0.5-ms duration were delivered to elicit twitch contractions. Tetanic contractions were elicited with 0.5-ms square wave pulses delivered in 350-ms trains. Frequency was increased until maximal force was attained. All subsequent tetanic contractions were elicited with the frequency that elicited maximal force, as described (13). All experiments were performed at room temperature (21–23°C). For data acquisition, a personal computer, a D-A and A-D board interface (Molecular Devices, Sunnyvale, CA), and pCLAMP software (Axon Instruments, Union City, CA) were used.

Dose-response curves were established for FDB fibers from both young and old mice. To check the viability of the cells and reproducibility of tetanic contraction, a reference trial of 50 tetanic contractions, set at 10-s intervals for 9 min, was performed. The cell was not further tested if a decline in tetanus at any time during this protocol was >10% of the initial amplitude. The test protocol was as follows: 1), three control maximal tetanic contractions set at 2-min intervals; 2), application of 100  $\mu\text{M}$  4-CmC; 3), washout of the drug; 4), series of tetanic contractions elicited at 2-min intervals until recovery of the maximal contraction force; and 5), application of the next 4-CmC concentration. Steps 2–4 were repeated, substituting progressively greater 4-CmC concentrations—200, 350, 500, 750, and 1000  $\mu\text{M}$ —in Step 2. As preliminary experiments with 2000  $\mu\text{M}$  4-CmC did not induce any further increase in force, this concentration was not systematically tested.

Intracellular  $\text{Ca}^{2+}$  mobilization in response to 1 mM 4-CmC was recorded in enzymatically dissociated FDB fibers. FDB muscles were treated with 2 mg/ml collagenase (Sigma, St. Louis, MO) in a shaking bath at 37°C. After 3 h of enzymatic treatment, they were dissociated into single fibers using Pasteur pipettes of different tip size. Contraction was prevented by incubating

the fibers in 50  $\mu\text{M}$  *N*-benzyl-*P*-toluene sulfonamide (BTS) for 30 min and then loading with the  $\text{Ca}^{2+}$  indicator Fura-FF via the patch pipette in the whole-cell configuration of the patch clamp. Fura-FF, a low-affinity  $\text{Ca}^{2+}$  indicator, was used because it is ratiometric and can measure peak intracellular  $\text{Ca}^{2+}$  in FDB fibers without saturating (18).  $\text{Ca}^{2+}$  fluorescence was recorded using a photomultiplier-based system provided with a random access monochromator (Ram X, PTI). Excitation and emission filters were set at 340/380 nm and 510 nm wavelength (Omega Optical, Brattleboro, VT), respectively. The relation between the fluorescence ratio  $R$  ( $F_{380}/F_{340}$ ) and  $\text{Ca}^{2+}$  concentration was calculated, as described (29).  $R_{\text{max}}$  (3.50) and  $R_{\text{min}}$  (0.29) were calculated in FDB fibers equilibrated with 0.02% saponin and 1 mM  $\text{Ca}^{2+}$  concentration or in cells incubated for 20–30 min in 10  $\mu\text{M}$  BAPTA AM. As a wide range of  $K_d$  values for  $\text{Ca}^{2+}$  has been reported in the literature (6.5  $\mu\text{M}$  (18), 19.2  $\mu\text{M}$  (30), 31.5  $\mu\text{M}$  (31), and 35  $\mu\text{M}$  (32)), we decided to calibrate the Fura-FF used for our experiments in the muscle fiber. A  $K_d$  value of 51  $\mu\text{M}$  was determined in vitro using microcapillaries, a  $\text{Ca}^{2+}$  calibration kit (Molecular Probes-Invitrogen, Carlsbad, CA), and a Fura-FF concentration of 10  $\mu\text{M}$ , as described previously (18). The explanation for this wide range of  $K_d$  values is not obvious.

### Whole-cell patch-clamp, confocal fluorescence imaging, and SR $\text{Ca}^{2+}$ release calculations

Enzymatically dissociated fibers (see above) were transferred to a small, flow-through Lucite chamber positioned on a microscope stage. Fibers were continuously perfused with the external solution (see below) using a push-pull syringe pump (WPI, Sarasota, FL). Only fibers exhibiting a clean surface and no contraction were used for electrophysiological recordings. Muscle fibers were voltage-clamped using an Axopatch-200B amplifier (Molecular Devices) in the whole-cell configuration of the patch-clamp technique (33). Patch pipettes were pulled from borosilicate glass (Boralex, WPI) using a Flaming Brown micropipette puller (P97, Sutter Instrument, Novato, CA) and then fire-polished to obtain electrode resistances ranging from 450 to 650 k $\Omega$ . In the cell-attached configuration, the seal resistance was in the range 1–4.5 G $\Omega$ , and in the whole-cell configuration, values ranged between 75 and 120 M $\Omega$  (34). The pipette was filled with the following solution (mM): 140 Cs-aspartate, 5 Mg-aspartate, 20 Cs<sub>2</sub>EGTA, and 10 HEPES (*N*-[2-hydroxyethyl]piperazine-*N'*-[2-ethanesulfonic acid]), and pH was adjusted to 7.4 with CsOH (34,35). The pipette solution also contained 500  $\mu\text{M}$  Oregon green bapta-5N (OGB-5N) (Invitrogen). The external solution contained (mM) 150 TEA (tetraethylammonium hydroxide)- $\text{CH}_3\text{SO}_3$ , 2  $\text{MgCl}_2$ , 2  $\text{CaCl}_2$ , 10 Na-HEPES, 0.05 BTS, and 0.001 tetrodotoxin (36,37). Solution pH was adjusted to 7.4 with CsOH. All the experiments were conducted at room temperature (21–22°C). For these experiments we preferred OGB-5N over Fura-FF due to its higher quantum yield and suitability for cell imaging with krypton-argon laser confocal microscopy. The fibers were loaded with OGB-5N via the patch pipette. The dye was allowed to diffuse for 20–30 min before fiber stimulation and after attaining the whole-cell voltage-clamp configuration. Intracellular OGB-5N transients were recorded using a Bio-Rad Radiance 2100 laser scanning confocal microscope (Zeiss, Oberkochen, Germany). Confocal microscopy allowed us to improve the signal/noise ratio under experimental conditions in which myoplasmic  $\text{Ca}^{2+}$  concentration was strongly buffered by 20 mM EGTA. The high EGTA concentration in the patch-pipette ensured a resting myoplasmic  $\text{Ca}^{2+}$  concentration value that approached the 60 nM existing in the pipette (20,38). This experimental manipulation also ensured a more accurate estimation of the  $\text{Ca}^{2+}$  release flux. Fibers were imaged through a C-Apochromat 40 $\times$  water-immersion objective (NA 1.2, Zeiss) or a 20 $\times$  Fluor (NA 0.75) using a krypton-argon laser at 488-nm excitation wavelength. The fluorescence emission was measured at  $528 \pm 25$  nm wavelength. For most experiments, the laser was attenuated to 6–12% with a neutral density filter. Fibers were imaged in line-scan (*x-t*) mode. The fiber was always oriented parallel to the *x* scan direction. Linescan images were acquired with 256 pixels (0.236  $\mu\text{m}/\text{pixel}$ ) in the *x*- and 512 pixels (0.833 ms/pixel) in the *t*-direction. For image acquisition, we used LaserSharp 2000 software (Bio-Rad, Zeiss), and for the analysis of the image intensity profile, Scion/Image J software (NIH, Bethesda, MD).

To determine the SR  $\text{Ca}^{2+}$  release flux,  $\text{Ca}^{2+}$  transients were analyzed using the closed-form equilibrium approximation (19) and a single-compartment kinetic model including EGTA, OGB-5N, and  $\text{Ca}^{2+}$  as the reactants with rate constants determined in vitro (20,21). The kinetics of the  $\text{Ca}^{2+}$  release flux ( $J(t)$ ) was described by the equation

$$J(t) = J_T(1 - e^{-(t/\tau_{\text{on1}})})^4 e^{-(t/\tau_{\text{off1}})} + J_S(1 - e^{-(t/\tau_{\text{on2}})}), \quad (1)$$

where  $J_T$  is the amplitude of a transient component of the total  $\text{Ca}^{2+}$  release flux and  $J_S$  is the amplitude of a steady component of the total  $\text{Ca}^{2+}$  release flux.

### OGB-5N calibration in vitro and in FDB mouse fibers

OGB-5N  $K_d$  for  $\text{Ca}^{2+}$  was calculated in vitro using borosilicate micropipettes (1.12 and 1.5 mm internal and external diameter, respectively) and a set of 11  $\text{Ca}^{2+}$  calibration standard solutions (Calbuf-2, WPI), containing 25  $\mu\text{M}$  OGB-5N.  $\text{Ca}^{2+}$  concentration in the standard solutions ranged from pCa 4 to 8, and their osmolality was 300 mOsm. The normalized fluorescence/pCa relationship was plotted, and a Hill equation fitted to data points ( $n = 6$ –10 pipettes/ $\text{Ca}^{2+}$  concentration). The calculated  $K_d$  value was 37  $\mu\text{M}$  for the batch of OGB-5N used. The in vivo calibration was carried out in enzymatically dissociated FDB fibers from young (4–6 months) mice. The fiber preparation followed the protocol described above for fluorescence recordings. Fibers were transferred to the recording chamber and exposed to 50  $\mu\text{M}$  BTS. We found that this concentration of the myosin II ATPase inhibitor completely suppresses contraction in fibers tested at optimal length (data not shown). Fibers were exposed to 0.02% saponin for 1 min and then to the  $\text{Ca}^{2+}$  standard solutions containing 25  $\mu\text{M}$  OGB-5N. This procedure allowed the intracellular compartment to equilibrate with the external medium. The maximal fluorescence intensity recorded in each fiber was computed for the dose-response curve. This analysis provided a  $K_d$  of 36  $\mu\text{M}$  ( $n = 15$ –24 fibers/ $\text{Ca}^{2+}$  concentration), which is consistent with the value obtained by in vitro calibration.

### STATISTICAL ANALYSIS

Data are presented as mean  $\pm$  SE, as indicated. Statistical significance among variables was determined using the parametric Student's *t*-test and Mann Whitney rank sum test run in SigmaPlot 8.0 or SigmaStat 3.0 (SPSS, Chicago, IL). Values of  $P < 0.05$  were considered significant.

## RESULTS

### 4-CmC concentration-force relationship in single intact FDB muscle fiber

The first group of experiments used 4-CmC as the agent to bypass sarcolemma and directly elicit massive SR  $\text{Ca}^{2+}$  release. Therefore, we defined potential differences in the drug's ability to evoke contractures at submaximal and maximal concentrations in single intact muscle fibers from young and old mice. Fiber contracture was elicited by various 4-CmC concentrations (100, 200, 350, 500, 750, and 1000  $\mu\text{M}$ ) and measured in single intact FDB fibers from young mice ( $n = 5$  fibers from three mice) and old mice ( $n = 6$  fibers from three mice). The single intact fiber preparation has

several advantages over a multifiber preparation. First, the contracting fiber can be very rapidly exposed to the perfusion solution. Second, whereas fibers can heterogeneously contribute to whole-muscle force production due to differences in pennation and length, we can be sure the single intact fiber is functioning at optimal length ( $L_0$ ) (6,39). Fig. 1 A shows force of contracture measured in a young, intact, skeletal FDB muscle fiber, activated by increasing concentrations of 4-CmC normalized to maximal force. Tetanic contractions fully recovered between increasing concentrations of 4-CmC. Application of 100  $\mu\text{M}$  4-CmC did not result in a significant force of contracture. The force of contracture steadily rose from 200  $\mu\text{M}$  to a maximum induced by 750–1000  $\mu\text{M}$  4-CmC that approximately equaled the amplitude of tetanic contraction (see below). Application of 1 mM 4-CmC elicited force similar to that obtained with 750  $\mu\text{M}$  but more reproducible. Concentrations  $> 1$  mM resulted in an incomplete tetanic recovery, indicating that 1 mM is the highest concentration of 4-CmC to accurately elicit maximal force of contracture without inducing damage. Fig. 1 B plots all data points for fibers from young and old mice, and curves are fitted using the equation

$$F/F_{\text{max}} = F_{\text{min}} + (F_{\text{max}} - F_{\text{min}})/(1 + (x/\text{EC}_{50})^n), \quad (2)$$

where  $F$  is force;  $x$  represents the 4-CmC concentration;  $\text{EC}_{50}$  is the 4-CmC concentration that elicits 50% of the maximum

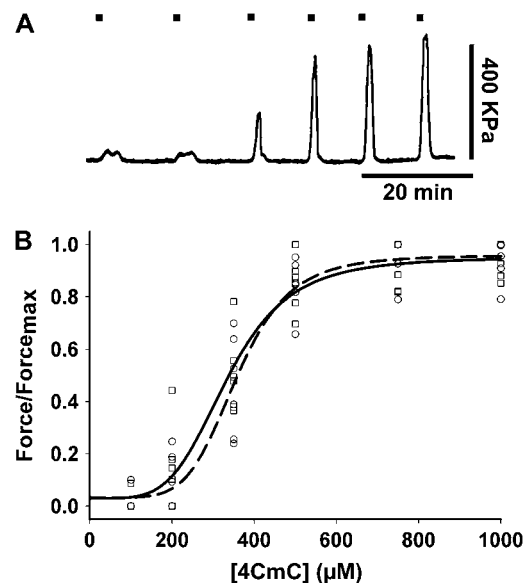


FIGURE 1 (A) 4-CmC dose-response curve in single intact FDB fibers from young and old mice. Contractures in single mouse FDB fibers in response to 100, 200, 350, 500, 750, and 1000  $\mu\text{M}$  4-CmC. Marks above indicate exposure time to the drug. (B) Normalized maximal force/4-CmC concentration relationship.  $\text{EC}_{50}$  calculated in fibers from young (circles) and old (squares) mice (in  $\mu\text{M}$ , mean  $\pm$  SE):  $335 \pm 16$  ( $n = 6$  fibers from five mice) and  $358 \pm 7$  ( $n = 6$  fibers from five mice), respectively, did not differ significantly ( $P > 0.05$ ). Data points represent individual fibers. Experimental points were fitted to a Hill equation. Solid and dashed lines are the fitting curves to data points for young and old mice, respectively.

response; and  $n$  is the Hill slope. The EC50 values for fibers from young and old mice were  $295 \pm 22$  and  $274 \pm 33 \mu\text{M}$ , respectively ( $P > 0.05$ ).

### FDB single intact fiber contracture/tetanus

The second set of experiments compared the force developed by a single intact fiber in response to 1 mM 4-CmC-induced contracture or depolarization-mediated maximal tetanus. Both types of responses were expressed as specific force, as described by Gonzalez et al. (6). The 4-CmC contracture recorded in fibers from young ( $n = 23$ ) and old ( $n = 8$ ) mice did not differ statistically; however, the tetanic responses induced by field stimulation resulted in significant specific force decrease in old ( $n = 16$ ) compared to young ( $n = 12$ ) mice (Fig. 2, A–D) ( $P < 0.05$ ). Fig. 2 E shows tetanic contraction and contracture specific force for all fibers from young and old mice studied. The age-dependent decline in fiber tetanic specific force confirms previous reports from our lab (6,13). In those publications, we also reported a decreased peak intracellular  $\text{Ca}^{2+}$  concentration recorded simultaneously with tetanic contraction. The 4-CmC-evoked  $\text{Ca}^{2+}$  release was recorded in enzymatically dissociated and BTS-immobilized FDB fibers from young ( $n = 8$ ) (Fig. 2 F a) and old ( $n = 7$ ) (Fig. 2 F b) mice, using Fura-FF as the ratiometric  $\text{Ca}^{2+}$  indicator. Fig. 2 G shows no statistically significant difference in the peak intracellular  $\text{Ca}^{2+}$  transient recorded in fibers from both age groups. Although these results do not rule out differences in SR  $\text{Ca}^{2+}$  content, they suggest that the age-dependent decline in electrically elicited fiber force cannot be explained by significant alterations in maximal SR-releasable  $\text{Ca}^{2+}$ .

### Direct measurement of SR $\text{Ca}^{2+}$ release in voltage-clamped FDB muscle fibers

Fig. 3 A illustrates OGB-5N transients in FDB fibers from young and old mice detected by confocal microscopy in linescan mode. Fibers were voltage-clamped at  $-90 \text{ mV}$  and depolarized by a command pulse to  $60 \text{ mV}$  for  $80 \text{ ms}$ . The pixel intensity profile superimposed on the images exhibits a peak that rapidly decays, followed by a “steady” phase until the end of fiber depolarization. The OGB-5N transient shape is similar to the SR  $\text{Ca}^{2+}$  release waveform obtained using a deductive mathematical algorithm (40,41). The amplitude of the peak and the steady phases of the OGB-5N transients are smaller in the old fiber than the young. Although the pulse duration in our regular protocol was  $40 \text{ ms}$  (see below), in this case, we prolonged the depolarizing pulse to better display differences in the “steady” phase between these recordings. Records in Fig. 3, A and B, were fitted and superimposed on the model equations, previously described (21), in fibers from young and old mice (Fig. 3, C and D, respectively, *dashed lines*). The time course of the predicted  $\text{Ca}^{2+}$  concentration closely matches that of the measured  $\Delta F/F$  fluorescence transients. The corresponding free  $\text{Ca}^{2+}$  concentrations were

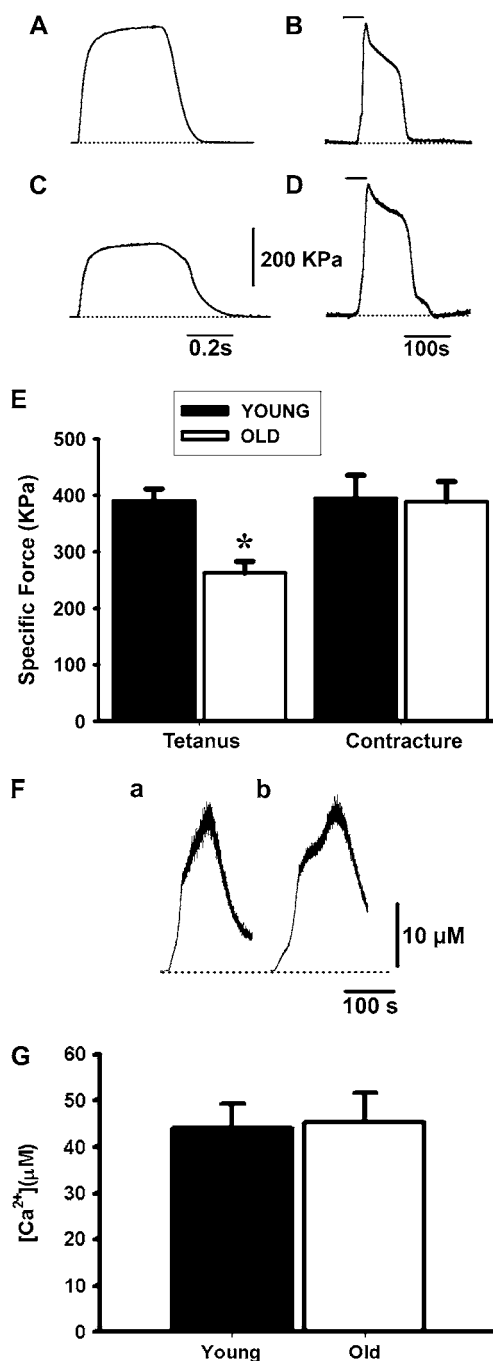


**FIGURE 2** Tetanus and 4-CmC contracture in FDB fibers. (A and C) Tetani recorded in single intact FDB fibers from young (A) and old (C) mice in response to a 350-ms-duration pulse (electrical field stimulation) at a frequency of 100 Hz. (B and D) 4-CmC contractures in fibers from young (B) and old (D) mice. The horizontal line above the curve indicates exposure time to the drug, and the dotted line is the baseline. (E) Specific force for tetanus and contracture in fibers from young and old mice expressed in kPa (mean  $\pm$  SE). The asterisk indicates a statistically significant difference in tetanus between age groups and between tetanus recorded in old mice compared to 4-CmC contractures in fibers from both young and old mice. (F) Intracellular  $\text{Ca}^{2+}$  transients evoked by 1 mM 4-CmC in fibers from young (a) and old (b) mice. The bars above indicate the time the fiber was exposed to the drug. (G) Statistical analysis of the peak intracellular  $\text{Ca}^{2+}$  concentration recorded in fibers from young ( $n = 8$  fibers) and old ( $n = 7$  fibers) mice.

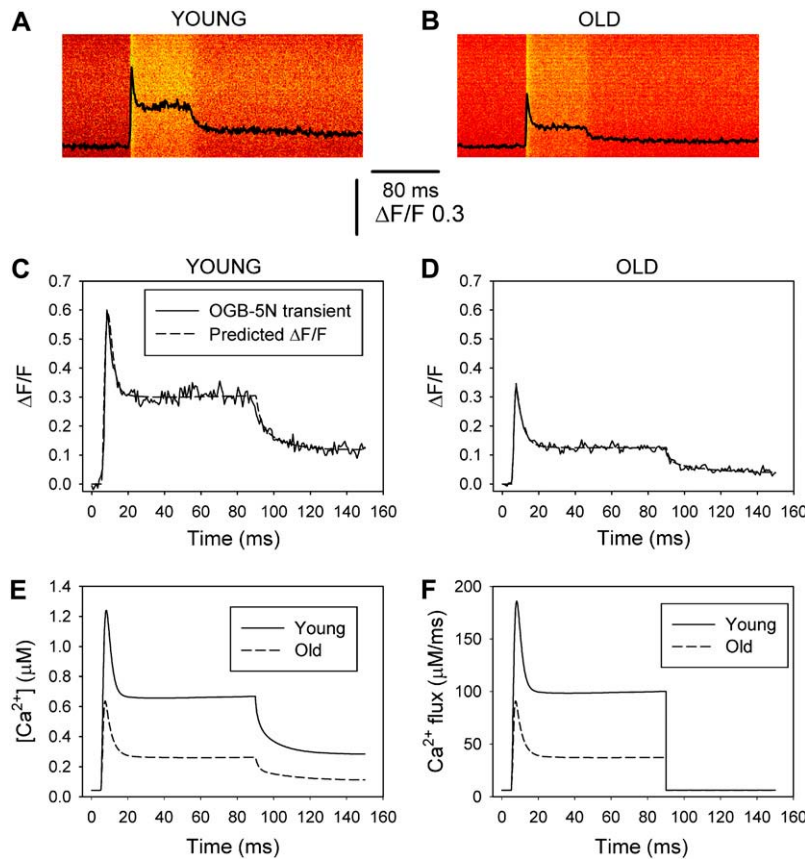


FIGURE 3 OGB-5N transients in FDB fibers from young and old mice. (A and B) OGB-5N fluorescence transients recorded in confocal linescan mode in whole-cell, patch-clamped FDB fibers in response to an 80-ms command pulse to 60 mV (holding potential,  $-90$  mV). The internal solution contained high EGTA (20 mM) and a low-affinity  $\text{Ca}^{2+}$  indicator (OGB-5N). (C and D) OGB-5N transients (solid lines) fitted to, and superimposed on, the predictions of the model equations (dashed lines) in fibers from young (C) and old (D) mice, respectively. (E and F) Free  $\text{Ca}^{2+}$  concentration and SR  $\text{Ca}^{2+}$  release flux corresponding to the fibers represented in A–D. The values for the kinetic parameters  $\tau_{\text{on1}}$  (ms),  $\tau_{\text{on2}}$  (ms), and  $\tau_{\text{off1}}$  (ms) were, respectively, 0.23, 0.025, and 2.4 for young mice, and 0.21, 0.029, and 2.7 for old mice.

calculated and represented in Fig. 3 E for the records depicted in Fig. 3, A–D. The calculated free  $\text{Ca}^{2+}$  concentration for the young fiber is similar to that previously reported for FDB fibers from young normal mice under similar experimental conditions (21), but obviously lower than in the presence of 0.2 mM EGTA in the pipette solution (9). Additionally, both free  $\text{Ca}^{2+}$  concentration and SR  $\text{Ca}^{2+}$  release flux are significantly lower in fibers from old compared to young mice. Experimental and theoretical  $\text{Ca}^{2+}$  transients exhibit a slow return to baseline (Fig. 3, C–E) during repolarization, which indicates that the rate of cytosolic  $\text{Ca}^{2+}$  removal by the SR and sarcolemmal  $\text{Ca}^{2+}$  transport mechanisms was negligible under these recording conditions (19). The predicted SR flux traces in Fig. 3 F, measured from the baseline, reach peak ( $J_T$ ) and steady ( $J_S$ ) values of 180 and 112  $\mu\text{M ms}^{-1}$ , respectively, for young mice, and 82 and 36  $\mu\text{M ms}^{-1}$  for old mice; the mean  $\pm$  SE of 12 fibers per age group were  $182 \pm 25$  and  $121 \pm 16 \mu\text{M ms}^{-1}$  for  $J_T$  and  $J_S$  in fibers from young and  $98 \pm 33$  and  $43 \pm 3.8 \mu\text{M ms}^{-1}$  for the same parameters in fibers from old mice. The 46% decrease in the peak  $\text{Ca}^{2+}$  flux ( $J_T$ ) closely matches the 48% reduction in the experimental  $\Delta F/F$  OGB-5N transients.

Fig. 4 shows the analysis of a complete set of recordings in fibers from young and old mice, voltage-clamped at  $-90$  mV ( $V_h$ ), and depolarized by command pulses from  $-60$  to 80

mV. Fig. 4 A compares OGB-5N transients at selected voltages from  $-30$  to 50 mV every 20 mV, the interval corresponding to the steepest part of the fluorescence-voltage curve (Fig. 4 B). The amplitudes of both peak and steady phases are lower in fibers from old compared to young mice. Fig. 4 B plots the peak OGB-5N transient recorded with a 10-mV interval in fibers from young and old mice. To analyze the voltage dependence of the OGB-5N signal, data points were fitted to a Boltzmann equation of the form

$$\Delta F/F = \Delta F/F_{\text{max}} / (1 + \exp((V_{1/2F} - V_m)/k)), \quad (3)$$

where  $\Delta F/F_{\text{max}}$  is the maximal normalized fluorescence;  $V_m$  is the membrane potential;  $V_{1/2F}$  is the half-activation potential; and  $k$  is the steepness of the curve.  $\Delta F/F_{\text{max}}$  was  $0.61 \pm 0.07$  and  $0.33 \pm 0.05$ ;  $V_{1/2F}$  was  $-14 \pm 1.2$  and  $-17 \pm 1.9$  mV; and  $k$  was  $13 \pm 1.2$  and  $14 \pm 1.5$ , for young ( $n = 35$  fibers) and old ( $n = 37$  fibers) mice, respectively. Differences between fibers from young and old mice are statistically significant ( $P < 0.05$ ) for  $\Delta F/F_{\text{max}}$ , but not for  $V_{1/2F}$  and  $k$ .

To determine whether differences in the peak and steady phases of SR  $\text{Ca}^{2+}$  release reported above depend on pulse duration, we recorded OGB-5N transients at 80 mV within a wide range of pulse durations (1.0, 2.5, 5.0, 10, 20, 40, 80, 100, and 200 ms) in fibers from young and old mice (Fig. 5, A and B). Differences in maximal OGB-5N transients were

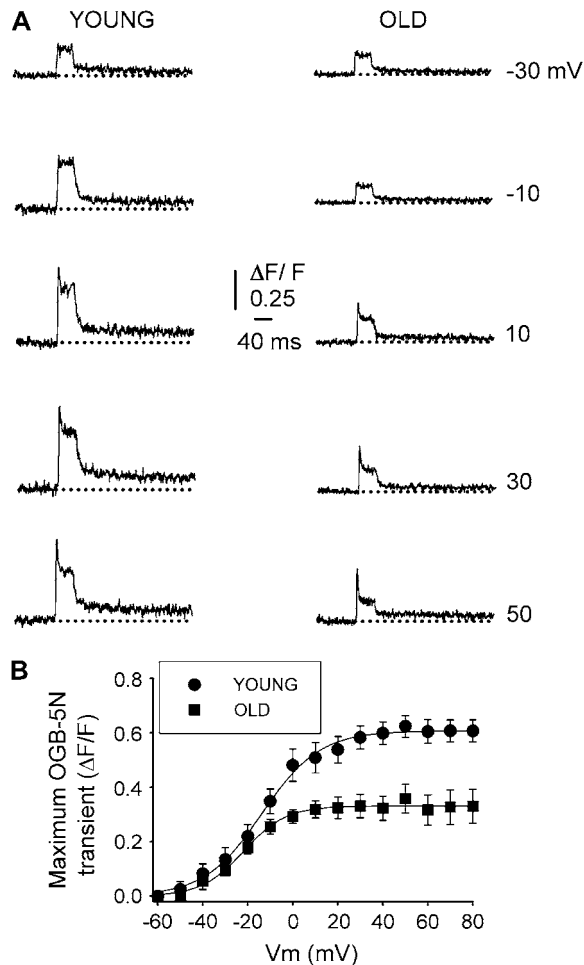


FIGURE 4 Voltage dependence of OGB-5N fluorescent signal in FDB fibers from young and old mice. (A) OGB-5N transients elicited by 40-ms command pulses at variable voltages. Traces illustrate the signal recorded at  $-30$ ,  $-10$ ,  $10$ ,  $30$ , and  $50$  mV. Dotted lines indicate the baseline. (B) Peak OGB-5N transient/ $V_m$  relationship in fibers from young (circles) and old (squares) mice. Data points were fitted to a Boltzmann equation of the form  $F = F_{\max}/(1 + \exp((V_{1/2} - V_m)/k))$ , where  $F_{\max}$  is the maximal fluorescence;  $V_{1/2}$  is the fluorescent half-activation potential;  $V_m$  is the membrane potential; and  $k$  is the steepness of the curve.  $F_{\max}$ , half-activation potential, and steepness of curves were, respectively,  $0.79$ ,  $-1.09$ , and  $3.37$  for young mice and  $0.39$ ,  $0.87$ , and  $2.25$  for old mice.

statistically significant within the whole range of pulse durations, which indicates that the age-dependent decline in SR  $\text{Ca}^{2+}$  release is not increased by prolonging RyR activation.

The peak and steady phases of the SR  $\text{Ca}^{2+}$  release waveform have been attributed to calcium- and voltage-mediated SR  $\text{Ca}^{2+}$  release, respectively (18,41–43). Fig. 5C represents the peak/steady ratio of traces recorded at  $50$  mV ( $40$ -ms duration) in fibers from young and old mice. Fibers from young mice ( $n = 25$ ) exhibit a shallow voltage dependence, as reported for rat fibers (44), and this relationship increases almost twofold in fibers from old mice ( $n = 27$ ). As both peak and steady phases of SR  $\text{Ca}^{2+}$  release are decreased in fibers from old compared to young mice (Fig. 4),

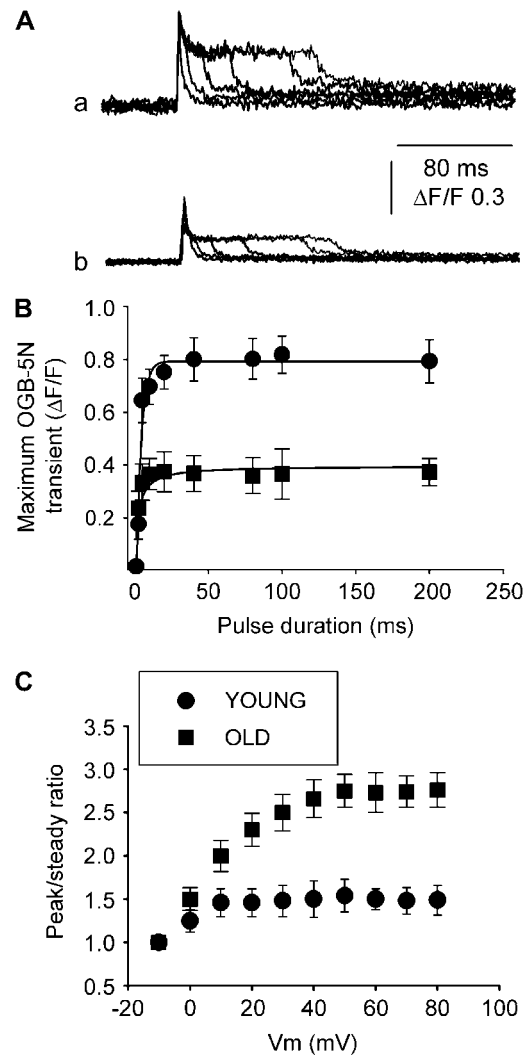
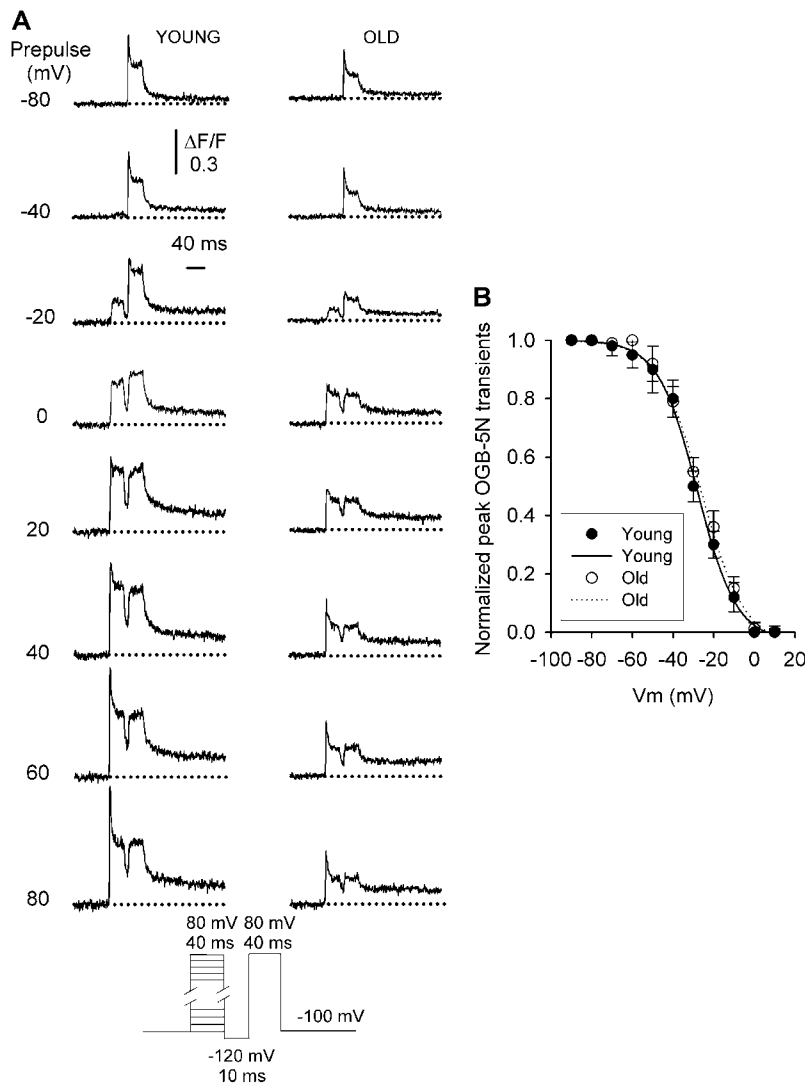


FIGURE 5 OGB-5N peak transient dependence on pulse duration and peak/steady ratio dependence on membrane voltage. Various pulse durations tested in fibers from young (Aa) and old (Ab) mice, voltage-clamped at  $-90$  mV (holding potential), and pulsed to  $80$  mV. (B) Maximum OGB-5N transient-pulse duration relationship in fibers from young (circles) and old (squares) mice. (C) Peak/steady ratio measured in OGB-5N transients in response to  $40$ -ms pulses.

a more pronounced decrease in the steady phase determines a significant increase in the peak/steady flux ratio. These results are consistent with the reported decrease in DHPR $\alpha 1$  subunit expression in aging mammalian skeletal muscle (5,45,46).

### $\text{Ca}^{2+}$ -dependent inactivation of SR $\text{Ca}^{2+}$ release in fibers from young and old mice

To determine whether the decreased SR  $\text{Ca}^{2+}$  flux results from an increase in  $\text{Ca}^{2+}$ -dependent inactivation of SR  $\text{Ca}^{2+}$  release with aging, we applied a double pulse protocol (Fig. 6A, bottom) (47–49). The peak or inactivating component of the test pulse was largest when very negative prepulses were applied. If the prepulse evoked measurable  $\text{Ca}^{2+}$  release, it



**FIGURE 6**  $\text{Ca}^{2+}$ -dependent inactivation of OGB-5N transients in fibers from young and old mice. A double-pulse protocol was used to explore  $\text{Ca}^{2+}$ -dependent inactivation of the OGB-5N transients (*bottom*). (*A*) OGB-5N transients elicited by prepulses from  $-80$  to  $80$  mV compared with  $20$ -mV intervals in FDB fibers from young and old mice. (*B*) Inactivation of the peak SR  $\text{Ca}^{2+}$  flux represented as a function of prepulse voltage in fibers from young and old mice. The peak component was normalized to the amplitude of the signal recorded in response to the prepulse to  $-100$  mV and fitted to a Boltzman equation (Eq. 4).

suppressed the inactivating component of the subsequent test pulse without affecting the steady phase. Fig. 6 *A* compares OGB-5N transients elicited by prepulses from  $-80$  to  $80$  mV with  $20$ -mV intervals in FDB fibers from young and old mice. The threshold for OGB-5N transients and suppression of the peak during the second pulse was  $-40$  mV and between  $-20$  and  $0$  mV, respectively, for fibers from young ( $n = 15$  fibers) and old ( $n = 17$  fibers) mice. Fig. 6 *B* represents inactivation of the peak SR  $\text{Ca}^{2+}$  flux as a function of prepulse voltage in fibers from young and old mice. The peak component was normalized to the amplitude of the signal recorded in response to the prepulse to  $-100$  mV (49) in fibers from young and old mice and fitted to a Boltzman equation of the form

$$\Delta F/F = \Delta F/F_{\max} / (1 + (\exp(-(V_{1/2F} - V_m)/k))), \quad (4)$$

where  $\Delta F/F_{\max}$  took a value of 1;  $V_m$  is the potential during the prepulse;  $V_{1/2F}$  is the half-inactivation potential; and  $k$  is the steepness of the curve.  $V_{1/2F}$  values were  $-28 \pm 3.2$  mV

and  $-25 \pm 2.9$  mV, and  $k$  values were  $9.6 \pm 1.2$  and  $10.7 \pm 1.4$  in fibers from young and old mice, respectively. No statistically significant differences were found for any of the inactivation parameters fitted to the experimental points ( $P > 0.05$ ). These results indicate that the age-dependent decline in SR  $\text{Ca}^{2+}$  release reported above is not accounted for by alterations in  $\text{Ca}^{2+}$ -dependent inactivation of SR  $\text{Ca}^{2+}$  flux.

## DISCUSSION

This work reports that 1), electrically evoked, but not 4-CmC-evoked, contraction produces significant differences in specific force recorded in fibers from old and young mice; 2), peak SR  $\text{Ca}^{2+}$  flux is reduced in fibers from old compared to young mice; 3), the steady component of SR  $\text{Ca}^{2+}$  flux decreases more markedly with aging than the peak SR  $\text{Ca}^{2+}$  release, and, therefore, the  $\text{Ca}^{2+}$  release flux peak/steady ratio is larger in old compared to young fibers; and 4),  $\text{Ca}^{2+}$ -

dependent inactivation of SR  $\text{Ca}^{2+}$  release does not differ between fibers from young and old mice. These results indicate that voltage-mediated SR  $\text{Ca}^{2+}$  release is impaired in fibers from old mice, and SR  $\text{Ca}^{2+}$  depletion does not seem to account for this effect, as the maximal SR-releasable  $\text{Ca}^{2+}$  does not differ in fibers from young and old mice.

### Voltage- and 4-CmC-evoked contraction in single intact fibers from young and old mice

This study took advantage of 4-CmC as a potent ryanodine receptor agonist (23,25,50) to investigate maximal releasable  $\text{Ca}^{2+}$  by measuring single-fiber specific force and peak intracellular  $\text{Ca}^{2+}$ . We tested a wide range of concentrations to examine age-dependent changes in fiber sensitivity to 4-CmC. Additionally, analysis of normalized force-[4-CmC] relationships suggests that the amount of  $\text{Ca}^{2+}$  released in response to maximal and submaximal 4-CmC concentrations is similar in fibers from young and old mice. It may be argued that fibers from aging mice exhibit lower SR  $\text{Ca}^{2+}$  release in response to 4-CmC, and the myofilaments' increased sensitivity for  $\text{Ca}^{2+}$  would offset the difference between young and old fibers. The literature does not support this speculation, because the  $\text{pCa}_{50}$  measured in skinned fibers from young adult and old mice was reported as 5.9 and 5.8, respectively (51). Peak intracellular  $\text{Ca}^{2+}$  recording, though not a direct measurement of SR  $\text{Ca}^{2+}$  release, indicates that the release flux is not altered when the ECC mechanism is bypassed. These results, together with the decreased tetanic force in response to electrical stimulation, indicate that voltage-mediated SR  $\text{Ca}^{2+}$  release, but not maximal SR-releasable  $\text{Ca}^{2+}$ , is impaired in aging muscle fibers. A recent study suggests that fragmented and uncoupled SR stores a  $\text{Ca}^{2+}$  pool sensitive to caffeine but not to sarcolemmal depolarization in aging muscle (52). However, segregated  $\text{Ca}^{2+}$  release is unlikely to explain our results, due to the fact that ultramicroscopic studies of mouse (53) or human muscle fibers do not report the presence of feet (RyR) beyond the SR junctional face (54).

### Direct measurement of SR $\text{Ca}^{2+}$ release in FDB fibers

The method used here to measure directly SR  $\text{Ca}^{2+}$  release has some advantages compared to those previously used (see below). High myoplasmic EGTA concentration prevents fiber movement, which is highly convenient for intracellular  $\text{Ca}^{2+}$  transient and sarcolemmal current recording with the patch-clamp technique. High EGTA also restricts the increase in myoplasmic free  $\text{Ca}^{2+}$  concentration to within a few hundred nanometers of the SR  $\text{Ca}^{2+}$  release sites (55). High concentration of this exogenous  $\text{Ca}^{2+}$  buffer dominates the endogenous buffer capacity of the fiber, and the SR  $\text{Ca}^{2+}$  release recordings become independent of intrinsic  $\text{Ca}^{2+}$  binding sites (19,20,55). Troponin C, parvalbumin, and

SERCA's  $K_d$  for  $\text{Ca}^{2+}$  are in the low micromolar–high nanomolar range, whereas EGTA's  $K_d$  for  $\text{Ca}^{2+}$  is in the low nanomolar range (17,55–57). The significant difference in  $\text{Ca}^{2+}$  affinity and the high myoplasmic concentration allow EGTA to overwhelm the endogenous buffer capacity (20,55).

SR  $\text{Ca}^{2+}$  release was measured in rat muscle fibers about a decade ago (14,15,44) and more recently in the mouse (17,18,49,58). These studies calculate  $\text{Ca}^{2+}$  release flux by applying an inductive (17) or deductive (41,59) mathematical approach to global intracellular  $\text{Ca}^{2+}$  transients. We used a method described in detail previously for cardiac myocytes and adult FDB muscle fibers (19,21) to investigate SR  $\text{Ca}^{2+}$  flux in aging muscle fibers. It takes advantage of the buffer capacity of high intracellular EGTA concentrations and the low affinity of the indicator OGB-5N for  $\text{Ca}^{2+}$ , and confocal microscopy can be used in the linescan mode. The  $\text{Ca}^{2+}$  input flux waveform we calculated resembles that reported using a  $\text{Ca}^{2+}$  removal model fit method in mouse (59), rat (44), and frog (12,41) fibers. A large, fast component, inactivated by a depolarizing prepulse, is followed by a smaller, sustained phase until the end of fiber depolarization (42). We did not detect a decline in the amplitude of this second phase of  $\text{Ca}^{2+}$  release flux, interpreted as SR  $\text{Ca}^{2+}$  depletion, in contrast to reports in the literature (60). More recently, an ~80% decrease in luminal  $\text{Ca}^{2+}$  content was recorded within 100 ms of membrane depolarization to 50 mV in mouse interosseus muscle (18). In this work, we did not observe a decline in the plateau phase of the  $\text{Ca}^{2+}$  release flux in FDB fibers subjected to prolonged depolarization (200 ms) (Fig. 5, A and B). It has been proposed that a strong  $\text{Ca}^{2+}$  flux through the DHPR in response to the increased driving force for  $\text{Ca}^{2+}$  upon fiber repolarization, which occurs at the  $\text{Ca}^{2+}$  tail current, transiently increases intracellular  $\text{Ca}^{2+}$  flux (19). We recorded intracellular  $\text{Ca}^{2+}$  flux in fibers in which SR calcium release was completely blocked by 30-min incubation in 5  $\mu\text{M}$  ryanodine, or  $\text{Ca}^{2+}$  flow through the DHPR was fully blocked with a combination of  $\text{La}^{3+}$  and  $\text{Cd}^{2+}$  added to the bath solution (34). These experiments recorded no contribution of the  $\text{Ca}^{2+}$  flux through the DHPR to intracellular  $\text{Ca}^{2+}$  (data not shown). Why we did not record the depletion reported previously is not obvious. We speculate that the Vaseline-gap voltage clamp applied to mammalian muscle fibers does not allow full recovery of SR  $\text{Ca}^{2+}$  content between pulses, probably due to the large dialysis of intracellular components through both ends of the fiber (34). However, this argument does not explain the decline in  $\text{Ca}^{2+}$  release flux recorded in mouse interosseus muscle fibers voltage-clamped with the two-microelectrode technique (18). Another speculation is that increasing cytosolic  $\text{Ca}^{2+}$  accumulation in response to prolonged depolarization in our high EGTA condition offsets the decline in the “steady” phase of the  $\text{Ca}^{2+}$  release flux. A function representing the increasing accumulation of myoplasmic  $\text{Ca}^{2+}$  concentration would be necessary to counterbalance SR  $\text{Ca}^{2+}$  depletion during a prolonged depolarization. However, the pioneer work by Pape and co-workers in cut frog



muscle fibers equilibrated with 20 mM EGTA showed a fast increase in free  $\text{Ca}^{2+}$  concentration near the SR  $\text{Ca}^{2+}$  release sites followed by a slow and sustained decay (55).

Values of  $\text{Ca}^{2+}$  release flux recorded here are comparable to those reported in the literature:  $\sim 200 \mu\text{M/ms}$  using fura-2 as the  $\text{Ca}^{2+}$  indicator in extensor digitorum longus (EDL) muscle fiber (17),  $\sim 200 \mu\text{M/ms}$  using Fura-FF in interosseus muscle fiber (18), and  $\sim 300 \mu\text{M/ms}$  using OGB-5N in FDB fibers (21). These values are almost fourfold higher than those reported in rat fibers (see Discussion in (18)).

### Differences in SR $\text{Ca}^{2+}$ release between fibers from young and old mice

Previous work from our laboratory showed a decrease in EDL, soleus (6), and FDB (13) muscle fiber SF with aging, and proposed that ECU explains it (61,62). Other theories have been proposed to account for the loss in SF; for example, contraction-induced injury (7) and posttranslational modifications of contractile proteins (8). Although contraction-induced injury has been reported in humans and reproduced in animal models after lengthening contractions, SF deficits have been recorded in the absence of this stress, which suggests that other mechanisms must be operating as well. The lack of SF alterations in manually skinned mouse EDL fibers (51,63) argues against the proposal that posttranslational modifications in aging muscle switch contractile proteins from strongly to weakly bound actomyosin (8). The ECU hypothesis is based on the age-dependent decrease in DHPR $\alpha 1$  subunit expression, charge movement, and intracellular  $\text{Ca}^{2+}$  transients (9,45); however, until now,  $\text{Ca}^{2+}$  release flux has not been directly measured in fibers from aging mice.

This study reports a decrease in the peak and steady components of SR  $\text{Ca}^{2+}$  flux in old compared to young fibers. The peak/steady-state ratio is larger in old than in young fibers and reflects a greater reduction in the steady than in the peak component. Similar differences have been reported for frog compared to rat muscle fibers (44). Whether changes in single RyR conductance among young and old fibers are significant and play a role in the decay in the SR  $\text{Ca}^{2+}$  flux is not known. Single-channel conductance has been measured only in RyR1 from young mammalian species (64) but not in aging muscle. The lower steady component of SR  $\text{Ca}^{2+}$  flux in old compared to young mice could result from lower values of DHPR $\alpha 1$  subunit density in the transverse tubule membrane, RyR1 density in the SR membrane, open probability for DHPR and/or RyR1, or  $\text{Ca}^{2+}$  driving force. In addition, channel mistargeting/triad disorganization in aging muscle (see below) could lead to impaired DHPR/RyR1 interaction. Decreased DHPR $\alpha 1$  subunit expression with aging has been reported in pooled muscles from rat (45), mouse (5), and rabbit (46). Persistent expression of this subunit in aged human skeletal muscle biopsy (65) raises concern about how representative a small muscle biopsy is of the whole musculature. No altera-

tions in RyR1 density have been reported in muscles from aging rat (45) or mouse (5). Open channel probability has not been recorded in either DHPR $\alpha 1$  subunit or RyR1 from aging mammals; therefore, we do not know whether it contributes to the decline in SR  $\text{Ca}^{2+}$  flux with aging. Potential alterations in driving force are difficult to assess, since SR  $\text{Ca}^{2+}$  content in muscle fibers from young and old mammals has not been measured, and, consequently, the  $\text{Ca}^{2+}$  gradient across the SR membrane is not known. However, the lack of significant difference between 4-CmC-evoked contracture amplitudes in single intact muscle fibers from young and old mice reported here suggests that the SR does not undergo significant  $\text{Ca}^{2+}$  depletion with aging.

The effect of depolarizing prepulses of various amplitudes on SR  $\text{Ca}^{2+}$  release flux was analyzed. Putative  $\text{Ca}^{2+}$ -dependent inactivation of SR  $\text{Ca}^{2+}$  release does not differ significantly in fibers from young and old mice; therefore, alterations in  $\text{Ca}^{2+}$ -dependent SR  $\text{Ca}^{2+}$  release inactivation cannot account for the smaller SR  $\text{Ca}^{2+}$  flux recorded in young versus old fibers.

A recent ultramicroscopic study supports the tenet that progressive disorganization of the ECC apparatus in aging human skeletal muscle may account for the decline in performance (54). This work reports disarrangement of the sarcotubular-SR membrane network, characterized by longitudinally oriented tubules, triads not correctly targeted at the I-A band junction, and a high frequency of dyads, together with a decreased number of triads per muscle fiber surface, which would lead to fewer  $\text{Ca}^{2+}$  release units (54). Disorganized and/or missing calcium release units might contribute to the decreased SR  $\text{Ca}^{2+}$  flux reported here.

In summary, only indirect information on SR  $\text{Ca}^{2+}$  release in skeletal muscle from senescent mammals existed until now. This study contributes direct quantification of 4-CmC- and voltage-evoked SR  $\text{Ca}^{2+}$  release in FDB fibers from young adult and senescent mice. These results indicate that voltage-mediated SR  $\text{Ca}^{2+}$  release is impaired in fibers from old mice, and that SR  $\text{Ca}^{2+}$  depletion does not account for this finding, as an extra pool of SR-releasable  $\text{Ca}^{2+}$  was mobilized in response to direct RyR1 activation by 4-CmC.

We are grateful to Dr. Julio Vergara (Department of Physiology, University of California at Los Angeles) for providing us with the single-compartment computer model and input on data analysis.

This study was supported by grants from the National Institutes of Health, National Institute on Aging (AG13934 and AG15820) and the Muscular Dystrophy Association to Osvaldo Delbono, and by the Wake Forest University Claude D. Pepper Older Americans Independence Center (P30-AG21332).

## REFERENCES

1. Dirks, A. J., and C. Leeuwenburgh. 2005. The role of apoptosis in age-related skeletal muscle atrophy. *Sports Med.* 35:473–483.
2. Karakelides, H., and K. Sreekumar Nair. 2005. Sarcopenia of aging and its metabolic impact. *Curr. Top. Dev. Biol.* 68:123–148.

3. Kandarian, S. C., and R. W. Jackman. 2006. Intracellular signaling during skeletal muscle atrophy. *Muscle Nerve*. 33:155–165.
4. Brooks, S. V., and J. A. Faulkner. 1988. Contractile properties of skeletal muscles from young, adult and aged mice. *J. Physiol.* 404:71–82.
5. Renganathan, M., M. L. Messi, and O. Delbono. 1998. Overexpression of IGF-1 exclusively in skeletal muscle prevents age-related decline in the number of dihydropyridine receptors. *J. Biol. Chem.* 273:28845–28851.
6. Gonzalez, E., M. L. Messi, and O. Delbono. 2000. The specific force of single intact extensor digitorum longus and soleus mouse muscle fibers declines with aging. *J. Membr. Biol.* 178:175–183.
7. Brooks, S. V., and J. A. Faulkner. 1990. Contraction-induced injury: recovery of skeletal muscles in young and old mice. *Am. J. Physiol.* 258:C436–C442.
8. Lowe, D. A., J. T. Surek, D. D. Thomas, and L. V. Thompson. 2001. Electron paramagnetic resonance reveals age-related myosin structural changes in rat skeletal muscle fibers. *Am. J. Physiol. Cell Physiol.* 280:C540–C547.
9. Wang, Z.-M., M. L. Messi, and O. Delbono. 2000. L-type Ca<sup>2+</sup> channel charge movement and intracellular Ca<sup>2+</sup> in skeletal muscle fibers from aging mice. *Biophys. J.* 78:1947–1954.
10. Schneider, M. F., and W. K. Chandler. 1973. Voltage dependent charge movement of skeletal muscle: a possible step in excitation-contraction coupling. *Nature*. 242:244–246.
11. Rios, E., and G. Brum. 1987. Involvement of dihydropyridine receptors in excitation-contraction coupling in skeletal muscle. *Nature*. 325:717–720.
12. Melzer, W., A. Herrmann-Frank, and H. C. Lüttgau. 1995. The role of Ca<sup>2+</sup> ions in excitation-contraction coupling of skeletal muscle fibres. *Biochim. Biophys. Acta*. 1241:59–116.
13. González, E., M. L. Messi, Z. Zheng, and O. Delbono. 2003. Insulin-like growth factor-1 prevents age-related decrease in specific force and intracellular Ca<sup>2+</sup> in single intact muscle fibres from transgenic mice. *J. Physiol.* 552:833–844.
14. Delbono, O., and E. Stefani. 1993. Calcium transients in single mammalian skeletal muscle fibres. *J. Physiol.* 463:689–707.
15. Garcia, J., and M. F. Schneider. 1993. Calcium transients and calcium release in rat fast-twitch skeletal muscle fibres. *J. Physiol.* 463:709–728.
16. Szentesi, P., V. Jacquemond, L. Kovacs, and L. Csernoch. 1997. Intramembrane charge movement and sarcoplasmic calcium release in enzymatically isolated mammalian skeletal muscle fibres. *J. Physiol.* 505:371–384.
17. Baylor, S. M., and S. Hollingworth. 2003. Sarcoplasmic reticulum calcium release compared in slow-twitch and fast-twitch fibres of mouse muscle. *J. Physiol.* 551:125–138.
18. Ursu, D., R. P. Schuhmeier, and W. Melzer. 2005. Voltage-controlled Ca<sup>2+</sup> release and entry flux in isolated adult muscle fibres of the mouse. *J. Physiol.* 562:347–365.
19. Song, L. S., J. S. Sham, M. D. Stern, E. G. Lakatta, and H. Cheng. 1998. Direct measurement of SR release flux by tracking 'Ca<sup>2+</sup> spikes' in rat cardiac myocytes. *J. Physiol.* 512:677–691.
20. Woods, C. E., D. Novo, M. DiFranco, and J. L. Vergara. 2004. The action potential-evoked sarcoplasmic reticulum calcium release is impaired in mdx mouse muscle fibres. *J. Physiol.* 557:59–75.
21. Woods, C. E., D. Novo, M. DiFranco, J. Capote, and J. L. Vergara. 2005. Propagation in the transverse tubular system and voltage dependence of calcium release in normal and mdx mouse muscle fibres. *J. Physiol.* 568:867–880.
22. Zorzato, F., E. Scutari, V. Tegazzin, E. Clementi, and S. Treves. 1993. Chlorocresol: an activator of ryanodine receptor-mediated Ca<sup>2+</sup> release. *Mol. Pharmacol.* 44:1192–1201.
23. Westerblad, H., F. H. Andrade, and M. S. Islam. 1998. Effects of ryanodine receptor agonist 4-chloro-m-cresol on myoplasmic free Ca<sup>2+</sup> concentration and force of contraction in mouse skeletal muscle. *Cell Calcium*. 24:105–115.
24. Choisy, S., C. Huchet-Cadiou, and C. Leoty. 1999. Sarcoplasmic reticulum Ca<sup>2+</sup> release by 4-chloro-m-cresol (4-CmC) in intact and chemically skinned ferret cardiac ventricular fibers. *J. Pharmacol. Exp. Ther.* 290:578–586.
25. Herrmann-Frank, A., M. Richter, and F. Lehmann-Horn. 1996. 4-Chloro-m-cresol: a specific tool to distinguish between malignant hyperthermia-susceptible and normal muscle. *Biochem. Pharmacol.* 52:149–155.
26. Herrmann-Frank, A., M. Richter, S. Sarkozi, U. Mohr, and F. Lehmann-Horn. 1996. 4-Chloro-m-cresol, a potent and specific activator of the skeletal muscle ryanodine receptor. *Biochim. Biophys. Acta*. 1289:31–40.
27. Payne, A. M., Z. Zheng, E. Gonzalez, Z. M. Wang, M. L. Messi, and O. Delbono. 2004. External Ca<sup>2+</sup>-dependent excitation-contraction coupling in a population of ageing mouse skeletal muscle fibres. *J. Physiol.* 560:137–157.
28. Lannergren, J., and H. Westerblad. 1987. The temperature dependence of isometric contractions of single, intact fibres dissected from a mouse foot muscle. *J. Physiol.* 390:285–293.
29. Grynkiewicz, G., M. Poenie, and R. W. Tsien. 1985. A new generation of Ca<sup>2+</sup> indicators with greatly improved fluorescence properties. Role of specific intracellular signaling pathways. *J. Clin. Invest.* 96:1473–1483.
30. Wokosin, D. L., C. M. Loughrey, and G. L. Smith. 2004. Characterization of a range of fura dyes with two-photon excitation. *Biophys. J.* 86:1726–1738.
31. Lomax, R. B., C. Camello, F. Van Coppenolle, O. H. Petersen, and A. V. Tepikin. 2002. Basal and physiological Ca<sup>2+</sup> leak from the endoplasmic reticulum of pancreatic acinar cells. Second messenger-activated channels and translocons. *J. Biol. Chem.* 277:26479–26485.
32. Barg, S., X. Ma, L. Eliasson, J. Galvanovskis, S. O. Gopel, S. Obermuller, J. Platzer, E. Renstrom, M. Trus, D. Atlas, J. Striessnig, and P. Rorsman. 2001. Fast exocytosis with few Ca<sup>2+</sup> channels in insulin-secreting mouse pancreatic B cells. *Biophys. J.* 81:3308–3323.
33. Hamill, O. P., A. Marty, E. Neher, B. Sakmann, and F. J. Sigworth. 1981. Improved patch-clamp techniques for high-resolution current recording from cells and cell-free patches. *Pflügers Arch.* 391:85–100.
34. Wang, Z. M., M. L. Messi, and O. Delbono. 1999. Patch-clamp recording of charge movement, Ca<sup>2+</sup> current and Ca<sup>2+</sup> transients in adult skeletal muscle fibers. *Biophys. J.* 77:2709–2716.
35. Adams, B. A., T. Tanabe, A. Mikami, S. Numa, and K. G. Beam. 1990. Intramembrane charge movement restored in dysgenic skeletal muscle by injection of dihydropyridine receptor cDNAs. *Nature*. 346:569–572.
36. Delbono, O. 1992. Calcium current activation and charge movement in denervated mammalian skeletal muscle fibres. *J. Physiol.* 451:187–203.
37. Delbono, O., M. Renganathan, and M. L. Messi. 1997. Regulation of mouse skeletal muscle L-type Ca<sup>2+</sup> channel by activation of the insulin-like growth factor-1 receptor. *J. Neurosci.* 17:6918–6928.
38. Pusch, M., and E. Neher. 1988. Rates of diffusional exchange between small cells and a measuring patch pipette. *Pflügers Arch.* 411:204–211.
39. Sugi, H. 1998. Current Methods in Muscle Physiology. Advantages, Problems and Limitations. Oxford University Press, New York.
40. Melzer, W., E. Rios, and M. F. Schneider. 1986. The removal of myoplasmic free calcium following calcium release in frog skeletal muscle. *J. Physiol.* 372:261–292.
41. Melzer, W., E. Rios, and M. F. Schneider. 1987. A general procedure for determining the rate of calcium release from the sarcoplasmic reticulum in skeletal muscle fibers. *Biophys. J.* 51:849–863.
42. Schneider, M. F., and B. J. Simon. 1988. Inactivation of calcium release from the sarcoplasmic reticulum in frog skeletal muscle. *J. Physiol.* 405:727–745.
43. Csernoch, L., V. Jacquemond, and M. F. Schneider. 1993. Microinjection of strong calcium buffers suppresses the peak of calcium release during depolarization in frog skeletal muscle fibers. *J. Gen. Physiol.* 101:297–333.
44. Shirokova, N., J. Garcia, G. Pizarro, and E. Rios. 1996. Ca<sup>2+</sup> release from the sarcoplasmic reticulum compared in amphibian and mammalian skeletal muscle. *J. Gen. Physiol.* 107:1–18.

45. Renganathan, M., M. L. Messi, and O. Delbono. 1997. Dihydropyridine receptor-ryanodine receptor uncoupling in aged skeletal muscle. *J. Membr. Biol.* 157:247–253.
46. Ryan, M., B. M. Carlson, and K. Ohlendieck. 2000. Oligomeric status of the dihydropyridine receptor in aged skeletal muscle. *Mol. Cell Biol. Res. Commun.* 4:224–229.
47. Delbono, O. 1995.  $\text{Ca}^{2+}$  modulation of sarcoplasmic reticulum  $\text{Ca}^{2+}$  release in rat skeletal muscle fibers. *J. Membr. Biol.* 146:91–99.
48. Garcia, J., and M. F. Schneider. 1995. Suppression of calcium release by calcium or procaine in voltage clamped rat skeletal muscle fibres. *J. Physiol.* 485:437–445.
49. Szentesi, P., L. Kovacs, and L. Csernoch. 2000. Deterministic inactivation of calcium release channels in mammalian skeletal muscle. *J. Physiol.* 528:447–456.
50. Choisy, S., C. Huchet-Cadiou, and C. Leoty. 2000. Differential effects of 4-chloro-m-cresol and caffeine on skinned fibers from rat fast and slow skeletal muscles. *J. Pharmacol. Exp. Ther.* 294:884–893.
51. Brooks, S. V., and J. A. Faulkner. 1994. Isometric, shortening, and lengthening contractions of muscle fiber segments from adult and old mice. *Am. J. Physiol.* 267:C507–C513.
52. Weisleder, N., M. Brotto, S. Komazaki, Z. Pan, X. Zhao, T. Nosek, J. Parness, H. Takeshima, and J. Ma. 2006. Muscle aging is associated with compromised  $\text{Ca}^{2+}$  spark signaling and segregated intracellular  $\text{Ca}^{2+}$  release. *J. Cell Biol.* 174:639–645.
53. Franzini-Armstrong, C. 1991. Simultaneous maturation of transverse tubules and sarcoplasmic reticulum during muscle differentiation in the mouse. *Dev. Biol.* 146:353–363.
54. Boncompagni, S., L. d'Amelio, S. Fulle, G. Fano, and F. Protasi. 2006. Progressive disorganization of the excitation-contraction coupling apparatus in aging human skeletal muscle as revealed by electron microscopy: a possible role in the decline of muscle performance. *J. Gerontol. A Biol. Sci.* 61:995–1008.
55. Pape, P. C., D. S. Jong, and W. K. Chandler. 1995. Calcium release and its voltage dependence in frog cut muscle fibers equilibrated with 20 mM EGTA. *J. Gen. Physiol.* 106:259–336.
56. Zot, H. G., and J. D. Potter. 1982. A structural role for the  $\text{Ca}^{2+}$ - $\text{Mg}^{2+}$  sites on troponin C in the regulation of muscle contraction. Preparation and properties of troponin C depleted myofibrils. *J. Biol. Chem.* 257:7678–7683.
57. Dode, L., B. Vilsen, K. Van Baelen, F. Wuytack, J. D. Clausen, and J. P. Andersen. 2002. Dissection of the functional differences between sarco (endo)plasmic reticulum  $\text{Ca}^{2+}$ -ATPase (SERCA) 1 and 3 isoforms by steady-state and transient kinetic analyses. *J. Biol. Chem.* 277:45579–45591.
58. Szentesi, P., C. Collet, S. Sarkozi, C. Szegedi, I. Jona, V. Jacquemond, L. Kovacs, and L. Csernoch. 2001. Effects of dantrolene on steps of excitation-contraction coupling in mammalian skeletal muscle fibers. *J. Gen. Physiol.* 118:355–375.
59. Schuhmeier, R. P., and W. Melzer. 2004. Voltage-dependent  $\text{Ca}^{2+}$  fluxes in skeletal myotubes determined using a removal model analysis. *J. Gen. Physiol.* 123:33–51.
60. Schneider, M. F., B. J. Simon, and G. Szucs. 1987. Depletion of calcium from the sarcoplasmic reticulum during calcium release in frog skeletal muscle. *J. Physiol.* 392:167–192.
61. Delbono, O., K. S. O'Rourke, and W. H. Ettinger. 1995. Excitation-calcium release uncoupling in aged single human skeletal muscle fibers. *J. Membr. Biol.* 148:211–222.
62. Delbono, O. 2002. Molecular mechanisms and therapeutics of the deficit in specific force in ageing skeletal muscle. *Biogerontology.* 3:265–270.
63. Plant, D. R., and G. S. Lynch. 2002. Excitation-contraction coupling and sarcoplasmic reticulum function in mechanically skinned fibres from fast skeletal muscles of aged mice. *J. Physiol.* 543:169–176.
64. Smith, J. S., T. Imagawa, J. Ma, M. Fill, K. P. Campbell, and R. Coronado. 1988. Purified ryanodine receptor from rabbit skeletal muscle is the calcium-release channel of sarcoplasmic reticulum. *J. Gen. Physiol.* 92:1–26.
65. Ryan, M., G. Butler-Browne, I. Erzen, V. Mouly, L. E. Thomell, A. Wernig, and K. Ohlendieck. 2003. Persistent expression of the  $\alpha 1\text{S}$ -dihydropyridine receptor in aged human skeletal muscle: implications for the excitation-contraction uncoupling hypothesis of sarcopenia. *Int. J. Mol. Med.* 11:425–434.